Plant Cell Tiss Organ Cult (2017) 131:75–88
DOI 10.1007/s11240-017-1263-y

ORIGINAL ARTICLE

Populus euphratica J3 mediates root K^+/Na^+ homeostasis by activating plasma membrane H^+-ATPase in transgenic Arabidopsis under NaCl salinity

Yinan Zhang[1] · Yang Wang[1] · Gang Sa[1] · Yuhong Zhang[1] · Jiayin Deng[1] · Shurong Deng[1] · Meijuan Wang[1] · Huilong Zhang[1] · Jun Yao[1] · Xiuying Ma[2] · Rui Zhao[1] · Xiaoyang Zhou[1] · Cunfu Lu[1] · Shanzhi Lin[1] · Shaoliang Chen[1]

Received: 23 February 2017 / Accepted: 30 June 2017 / Published online: 10 July 2017

Abstract NaCl induced *PeJ3* (a *DnaJ* homolog) expression in *Populus euphratica* cell cultures. In contrast, salt treatment inhibited transcription of a J3-interacting protein kinase gene, *PePKS5* (Salt Overly Sensitive 2-Like Protein Kinase 5). To clarify the mechanism by which PeJ3 conferred salinity tolerance, we isolated *PeJ3* from *P. euphratica* and transformed it into Arabidopsis. *PeJ3* overexpression inhibited *AtPKS5* expression, but had no effect on *AtJ3* transcripts. After 10-day exposures to 100 mM NaCl, *PeJ3*-transgenic lines showed prolonged survival (40–54.4%) and longer roots (43.8–51.1%) compared to wild-type (WT) and vector control (VC) plants. The observed differences in salt acclimation between transgenic and WT depended on their ability to exclude Na^+ and maintain intracellular K^+. *PeJ3*-transgenic Arabidopsis accumulated less Na^+ in root cells, due at least in part, to the high Na^+ efflux in roots. K^+ flux recordings revealed that *PeJ3*-transgenic lines lost less K^+ than WT and VC under salt stress. In vitro and in vivo activity assays revealed that *PeJ3*-overexpression upregulated plasma membrane H^+-ATPase activity and enhanced H_2O_2 signaling in salt-stressed Arabidopsis. Consequently, *PeJ3*-transgenic plants retained high H^+-pumping activity under NaCl salinity, which contributed to K^+/Na^+ homeostasis in roots. In conclusion, *PeJ3* overexpression resulted in H^+-ATPase activation through transcriptional *AtPKS5* suppression and/or interactions with AtPKS5 kinase. Under salinity stress, upregulated H^+-pumps (i) promoted Na^+/H^+ exchange across the Arabidopsis plasma membrane, (ii) reduced K^+ efflux mediated by depolarization-activated plasma membrane channels, and (iii) stimulated H_2O_2 signaling, which increased cytosolic free Ca^{2+} and stimulated Na^+ extrusion through Salt Overly Sensitive signaling in Arabidopsis.

Keywords *Populus euphratica* · *DnaJ* homolog 3 · PM H^+-ATPase · NaCl · PKS5 · H_2O_2 · Arabidopsis · Ion flux · NMT

Communicated by Henryk Flachowsky.

Yinan Zhang, Yang Wang, and Gang Sa have contributed equally to this work.

Electronic supplementary material The online version of this article (doi:10.1007/s11240-017-1263-y) contains supplementary material, which is available to authorized users.

✉ Shaoliang Chen
Lschen@bjfu.edu.cn

[1] Beijing Advanced Innovation Center for Tree Breeding by Molecular Design, College of Biological Sciences and Technology (Box 162), Beijing Forestry University, Beijing 100083, People's Republic of China

[2] Department of life Science and Engineering, Jining University, Qufu 273155, Shandong, People's Republic of China

Introduction

H^+-ATPases located in the plasma membranes (PMs) of plants and fungi sustain an H^+ gradient to drive the transport of minerals and metabolites (Palmgren 2001). The PM H^+-pumps play vital roles in signal transduction, cell expansion, plant development, stomatal opening, and salt response (Palmgren 2001; Roberkleber et al. 2003; Merlot et al. 2007; Sun et al. 2010a, b). In plant cells, PM H^+-ATPases contribute to maintaining ionic homeostasis in saline environments. Salt-resistant plants possess a great capacity for H^+ pumping activity, which enables salinized cells to retain K^+/Na^+ homeostasis and avoid ionic

toxicity (Hasegawa et al. 2000; Blumwald et al. 2000; Zhu 2001, 2003, 2016; Apse and Blumwald 2007; Munns and Tester 2008). Activated PM H^+-pumps counteract salt-activated K^+ efflux, which is mediated by depolarization-activated (DA) channels, e.g., outward rectifying K^+ channels (KORCs) and non-selective cation channels (NSCCs) (Chen et al. 2005, 2007; Shabala et al. 2006; Britto and Kronzucker 2008). It is particularly important for plant cells to maintain their capacity for Na^+ exclusion under NaCl stress conditions (Munns and Tester 2008). Na^+ extrusion is mainly driven by H^+-ATPases in the PM (Morsomme and Boutry 2000; Akbari and Labeau 2003; Chen et al. 2007; Munns and Tester 2008; Ding et al. 2010). Previous studies revealed that upregulated H^+-ATPases promoted the exchange of Na^+ with H^+ across the PM (Blumwald et al. 2000; Zhu 2003; Sun et al. 2009a, 2010b). Furthermore, PM H^+-ATPases were shown to accelerate H_2O_2 production by activating NADPH oxidases (Foreman et al. 2003; Kwak et al. 2003; Mittler et al. 2004; Moshe and Robert 2006; Chung et al. 2008; Sun et al. 2010b). It was found that H_2O_2 triggered Ca^{2+} influx through the *P. euphratica* PM, which led to elevated cytosolic Ca^{2+} concentrations (Sun et al. 2010b). Subsequently, elevated Ca^{2+} levels activated the Salt Overly Sensitive signaling pathway, which then activated the PM Na^+/H^+ antiporter (Shi et al. 2000, 2003; Ottow et al. 2005; Wu et al. 2007; Sun et al. 2009b).

PM H^+-ATPases are regulated by both transcriptional and post-translational pathways (Akbari and Labeau 2003). Genes that encode H^+-ATPases are modulated by a number of environmental factors, including salinity (Ding et al. 2010), hormones (Frías and Serrano 1996; Kim et al. 2001), mechanical stress (Oufattole and Boutry 2000), blue light (Zhang et al. 2004), and fungal elicitors (Xing et al. 1997). Apart from transcriptional regulation, PM H^+-ATPases may undergo rapid post-translational modulation (Janicka-Russak 2011). The phosphorylation of the C-terminal auto-inhibitory domain of the H^+-ATPase induces it to form a complex with a positive regulator, 14-3-3 protein (Palmgren et al. 1991; Camoni et al. 2000; Svennelid et al. 2000; Gévaudant et al. 2007). Conversely, in Arabidopsis, the PKS5 kinase inhibits H^+-pumping activity by directly phosphorylating the C-terminal regulatory domain (AHA2 isoform), which interferes with the interaction between AHA2 and the 14-3-3 protein (Fuglsang et al. 2007). A recent study showed that an Arabidopsis chaperone, DnaJ homolog 3 (a heat shock protein 40-like protein), interacted with PKS5 kinase to regulate the activity of the PM H^+-ATPase (Yang et al. 2010).

DnaJ/Hsp40 acts as an independent chaperone (Laufen et al. 1999). DnaJ proteins generally consist of a J-domain, a G/F-domain, a zinc finger (CxxCxGxG) domain, and a C-terminal sequence (Caplan et al. 1993; Silver and Way 1993). Under stress conditions, DnaJ assists with the folding, assembly, and translocation of proteins (Boston et al. 1996; Waters and Vierling 1996; Wang et al. 2004). In Arabidopsis, *AtJ3* is widely expressed in roots and above-ground organs, where transcription can be altered by water and temperature stress (Zhou and Miernyk 1999; Li et al. 2005). AtJ3 possesses all the essential domains of J-domain proteins (Zhou and Miernyk 1999). Some evidence has shown that PM H^+-ATPase activity is modulated by the activity of a chaperone J3, which inactivates PKS5 kinase in Arabidopsis (Yang et al. 2010). In this study, we found that NaCl increased *PeJ3* transcription in *P. euphratica* leaves (Supplemental Fig. 1). To clarify the function of PeJ3 in plant salt tolerance, we cloned *PeJ3* from *P. euphratica* and introduced it into the model plant, Arabidopsis. We found that *PeJ3* overexpression positively regulated PM H^+-ATPase in transgenic lines. Flux recordings with microelectrodes revealed that upregulated H^+-pumps benefited salinized roots by extruding Na^+ and by reducing K^+ loss through depolarization-activated channels in the PM. Consequently, transgenic plants that overexpressed *PeJ3* could maintain K^+/Na^+ homeostasis during a period of salinity stress.

Materials and methods

Plants, cell culture, and NaCl treatment

Populus euphratica seedlings were obtained from Bayin'guoleng Mongol Autonomous Prefecture of Xinjiang. In April, seedlings were planted in 10-L pots containing a mixture of sand:soil (1:1). The potted seedlings were placed in a greenhouse at Beijing Forestry University (BJFU), China. Plants were well irrigated and fertilized with full-strength Hoagland's nutrient solution, as previously described (Sun et al. 2009a, b). After 3 months of culture, uniform seedlings were subjected to 24 h of increasing NaCl stress, by top watering with 2 L of 50 and 100 mM NaCl in full-strength Hoagland's nutrient solution. The 50 mM solution was applied at the first 3 h, and then plants were left standing in the final concentration of NaCl until the end of experiment (Ding et al. 2010). After 0, 12, and 24 h of salt treatment, mature leaves were collected from the upper shoots. The age of these fully expanded leaves was 25–30 days. The sampled leaves were immediately frozen in liquid N_2 until processing for real-time quantitative PCR (RT-qPCR) assays (described below).

Populus euphratica calli were generated from shoots, propagated, and subcultured, as previously described (Sun et al. 2010a, b). Callus cultures (ca 1.0 g fresh weight) were exposed to 100 mM NaCl in liquid Murashige and Skoog (MS) medium. The calli were suspended in liquid MS medium supplemented with or

without NaCl. The solutions were continuously aerated during the period of hydroponic treatment. Then, after 0, 12, and 24 h of treatment, the no-salt control and salinized cells were collected and frozen in liquid N_2 until processing for RT-qPCR assays.

Arabidopsis thaliana (Columbia, Col-0) plants were used for salt tests and transgene experiments. Seeds were germinated on 1/2 MS solid medium supplemented with 0.24% Phytagel (Sigma-Aldrich; Wang et al. 2013b). Photosynthetically active radiation was maintained at 100 µmol m^{-2} s^{-1} during a long-day photoperiod (16-h). Seedlings were raised at 22 ± 1 °C with 70–80% relative humidity.

Cloning the *PeJ3* gene and sequence analysis

A Plant RNA Kit (QBio Technologies Inc., Beijing, China) was used to isolate total RNA from *P. euphratica* leaves. cDNA was synthesized from 1 µg total RNA with the Superscript III first-strand synthesis system (Invitrogen). A homologous *J3* sequence of *P. trichocarpa* (NCBI accession no. XM_ 002316443.2) was used to design primers. The primer sequences (5′–3′) were, as follows: forward, ATGTTTGGGAGAGCACCAA; reverse, TTATTGCTG AGCACATTGCAC. The purified PCR products were cloned into the pMD18-T vector for sequencing. A 1269-bp cDNA was identified as the full-length *PeJ3* transcript.

We performed protein multiple sequence alignments with ClustalW (http://www.genome.jp/tools/clustalw/). The phylogenetic tree was determined with MEGA5.0 software (http://www.megasoftware.net/index.php).

Generation of transgenic Arabidopsis plants that expressed *PeJ3*

The full-length open reading frame of *PeJ3* was cloned into the *pCAMBIA2300* vector (kanamycin resistance) between the *BamHI* and *SalI* sites. Transcription was driven by the cauliflower mosaic virus 35S (*CaMV 35S*) promoter. The constructs were then transformed to *Agrobacterium tumefaciens* strain *GV3101*, and finally introduced into *A. thaliana* (Clo-0) with the floral dip method (Clough and Bent 1998). Vector control (VC) *A. thaliana* plants were transformed with the blank *pCAMBIA2300* vector. T2 seeds were screened on 1/2 MS medium with 100 mg/L kanamycin. The antibiotic-resistant plants were grown in nutrient soil to obtain homozygous T3 seeds. The transgene expression levels of six T3 homozygous lines (OE1-3, 6, 10, and 11) were quantified with semi-quantitative reverse transcription PCR and RT-qPCR. Based on the transcript abundance of *PeJ3*, two positive transgenic lines, OE1 and OE2, were selected for further salt exposure experiments.

Semi-quantitative reverse transcription PCR and RT-qPCR

Total RNA was isolated from transgenic seedlings and wildtype (WT) Arabidopsis (10-day-old) with Trizol reagent (Invitrogen). Based on the manufacturer's instructions, RNA (1 µg) was used for reverse transcription with Moloney Murine Leukemia Virus (M-MLV) reverse transcriptase and an oligo (dT) primer (Promega, Madison, WI, USA). The cDNA products were used for semi-quantitative reverse transcription PCR amplification. The *PeJ3*-specific forward and reverse primers were: 5′-CACTCTGTG GCTTCCAGTTC-3′ and 5′-TTCATCAAGCTCCATGTC AGT-3′ (Supplemental Table 1). *Atactin2* was amplified as an internal control, with the following primers: forward, 5′-CTAAGCTCTCAAGATCAAAGGCTTA-3′; reverse, 5′-ACTAAAACGCAAAACGAAAGCGGTT-3′ (Supplemental Table 1). The thermocycling conditions for semi-quantitative reverse transcription were: 95 °C for 5 min → 28 cycles at: 95 °C for 30 s → 55 °C for 30 s → 72 °C for 30 s, finally at 72 °C for 7 min.

For RT-qPCR, total RNA was isolated from 10-day-old Arabidopsis seedlings and *P. euphratica* cell cultures with Trizol reagent (Invitrogen). The gene-specific forward and reverse primers used for *J3* and *PKS5* in *P. euphratica* (*PeJ3* and *PePKS5*) and Arabidopsis (*AtJ3* and *AtPKS5*) are shown in Supplemental Table 1. We used Arabidopsis *Atactin2* and *AtEF1α* genes and *P. euphratica PeACT2* and *PeACT7* (Han et al. 2013; Shen et al. 2013, 2015) genes as internal controls. PCR was performed in a total volume of 25 µL, containing 0.3 µL forward and reverse primers (10 µM), 2 µL cDNA product, 1 U Ex Taq polymerase (Takara, Dalian, China), 2.5 µL 10× Ex Taq buffer, 0.4 µL dNTP mixture (2.5 mM) and 1.25 µL SYBR Green (Takara, Dalian, China) (Shen et al. 2015). The thermocycling conditions for RT-qPCR were: 95 °C for 5 min → 35 cycles at 95 °C for 30 s → 55 °C for 30 s → 72 °C for 30 s, finally at 72 °C for 10 min. The expression data for *PeJ3, PePKS5, AtJ3*, and *AtPKS5* were normalized to the expression level of each internal control with the $2^{-\Delta\Delta Ct}$ method (Livak and Schmittgen 2001).

Salt tolerance tests for transgenic lines

Salt tolerance assays were performed in plates with 1/2 MS medium. The disinfected seeds of WT, VC, and *PeJ3*-transgenic plants (PeJ3-OE1 and PeJ3-OE2) were grown in 1/2 MS medium in the presence or absence of 100 mM NaCl. Root lengths and survival rates were examined and photographed after 10 days of NaCl treatment. A parallel experiment was performed with KCl instead of NaCl to separate any potential conflation with osmotic effects.

In vitro assays for evaluating PM H^+-ATPase activity

With the aqueous two-phase partitioning method (Larsson et al. 1987), plasma membrane vesicles were isolated from 4-week-old WT, VC, and *PeJ3*-transgenic Arabidopsis (OE1 and OE2) plants. Hydrolysis activity of the PM H^+-ATPase was evaluated by measuring the inorganic phosphate (Pi) released from ATP (Ohnishi et al. 1975; Wang et al. 2013b).

Na^+ and K^+ flux recordings in roots

Seedlings that carried WT, VC, PeJ3-OE1, and PeJ3-OE2 constructs were grown on 1/2 MS solid medium for 7 days, then subjected to 0 or 100 mM NaCl in 1/2 MS liquid solution for 12 h. After 20 min of equilibration in measuring solution (0.5 mM KCl, 0.1 mM $CaCl_2$, 0.1 mM $MgCl_2$, 0.1 mM NaCl, and 2.5% sucrose, pH 5.8), steady-state fluxes of Na^+ and K^+ were recorded continuously for 30 min at the meristematic region, approximately 200 μm from the tip (Wang et al. 2013b; Han et al. 2014). The flux recordings were performed with the Non-invasive Micro-test Technique (NMT), as previously described (Sun et al. 2009a, b; Li et al. 2012; Lu et al. 2013; Wang et al. 2013b; Zhao et al. 2016). In this study, the Na^+ concentration was 0.1 mM in the measuring solution, because Na^+ fluxes were only recorded at low Na^+ concentrations with the Na LIX (Fluka 71178; Sun et al. 2009a, b; Li et al. 2012; Lu et al. 2013). In the measuring solution, Ca^{2+} and K^+ were set to low concentrations, 0.1 and 0.5 mM, respectively, to reduce interference with the Na^+ electrodes of the Na LIX (Fluka 71178; Cuin et al. 2011; Li et al. 2012).

H^+ flux recordings and in vivo assays of PM H^+-ATPase activity

With the NMT, we recorded the transient kinetics of H^+ in response to NaCl shock (100 mM), as previously reported (Sun et al. 2009b). To perform in vivo measurements of H^+-ATPase activity in the root PM, a PM H^+-ATPase inhibitor (sodium vanadate) was used to inhibit the H^+-pumping activity under NaCl stress (Sun et al. 2010b; Wang et al. 2013b). We treated 7-day-old seedlings of WT, VC, PeJ3-OE1, and PeJ3-OE2 with 500 μM vanadate for 30 min. Thereafter, roots were equilibrated for 15–20 min in the measuring solution (Sun et al. 2009a, b, 2010b). Then, transient H^+ kinetics were recorded in response to NaCl shock (100 mM) for 20 min in the inhibitor-pretreated roots.

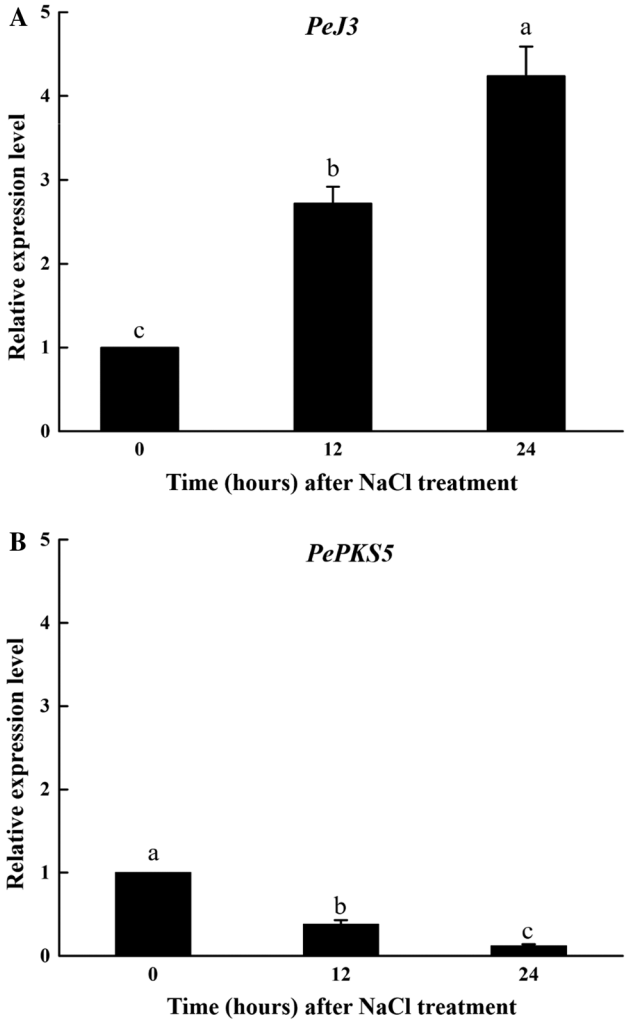

Fig. 1 Time dependence of gene expression in *Populus euphratica* callus cultures during NaCl stress. *P. euphratica* calli were salinized with 100 mM NaCl for 24 h. After 0, 12, and 24 h of salt treatment, total RNA was extracted from these cells and used for RT-qPCR assay. At different times, expression levels of **A** *PeJ3* and **B** *PePKS5* were measured relative to the *P. euphratica* housekeeping gene, *PeACT7*, an internal control. Primers designed to target genes, *PeJ3* and *PePKS5*, were based on the *P. euphratica* homologs that obtained from the NCBI database (http://www.ncbi.nlm.nih.gov/). The specific forward and reverse primers for *PeJ3, PKS5*, and *PeACT7* are listed in Supplemental Table 1. *Each column* is the mean of three independent experiments and *bars* represent the standard error of the mean. *Columns labeled with different letters* (*a, b*, and *c*) denote significant differences ($P < 0.05$) between treatment times

H_2O_2 production within root cells

A specific fluorescent probe, 2′,7′-dichlorodihydro fluorescein diacetate (H_2DCF-DA; Molecular Probes, Eugene, OR, USA) was used to examine H_2O_2 accumulation within root cells. Seedlings of WT, VC, PeJ3-OE1, and PeJ3-OE2 (7-day-old) were exposed to 0 or 100 mM NaCl for 10 min. Then, roots were incubated with 10 μM H_2DCF-DA

(prepared in 1/2 MS liquid solution, pH 5.7) in the dark for 5 min, followed by washing with 1/2 MS liquid solution (3–4 times). DCF-specific fluorescence was examined under a Leica SP5 confocal microscope (Leica Microsystems GmbH, Wetzlar, Germany), with excitation at 488 nm and emission at 510–530 nm. Relative fluorescence intensity was analyzed quantitatively with the Image-Pro Plus 6.0 (Sun et al. 2010a, b, 2012; Wang et al. 2013b).

Detection of cytosolic Na^+ concentrations

Cellular Na^+ concentrations in roots were detected with a Na^+-specific fluorescent probe, CoroNa™ Green, AM (Invitrogen, Carlsbad, CA, USA). Seedlings of WT, VC, PeJ3-OE1, and PeJ3-OE2 (7-day-old) were exposed to 0 or 100 mM NaCl in 1/2 MS liquid solution for 12 h. Thereafter, control and salinized plants were stained with CoroNa in the dark for 1 h, followed by 3–4 washes with distilled water. Na^+-fluorescence in the probe-loaded roots was determined with a Leica SP5 confocal microscope (excitation: 488 nm, emission: 510–530 nm; Sun et al. 2010a, b, 2012; Wang et al. 2013b). Image-Pro Plus 6.0 was used to quantify relative fluorescence intensity (Sun et al. 2010a, b, 2012; Wang et al. 2013b).

Data analysis

All experimental data were analyzed with SPSS version 17.0 software for statistical evaluations. Differences were considered significant at $P < 0.05$, unless otherwise stated.

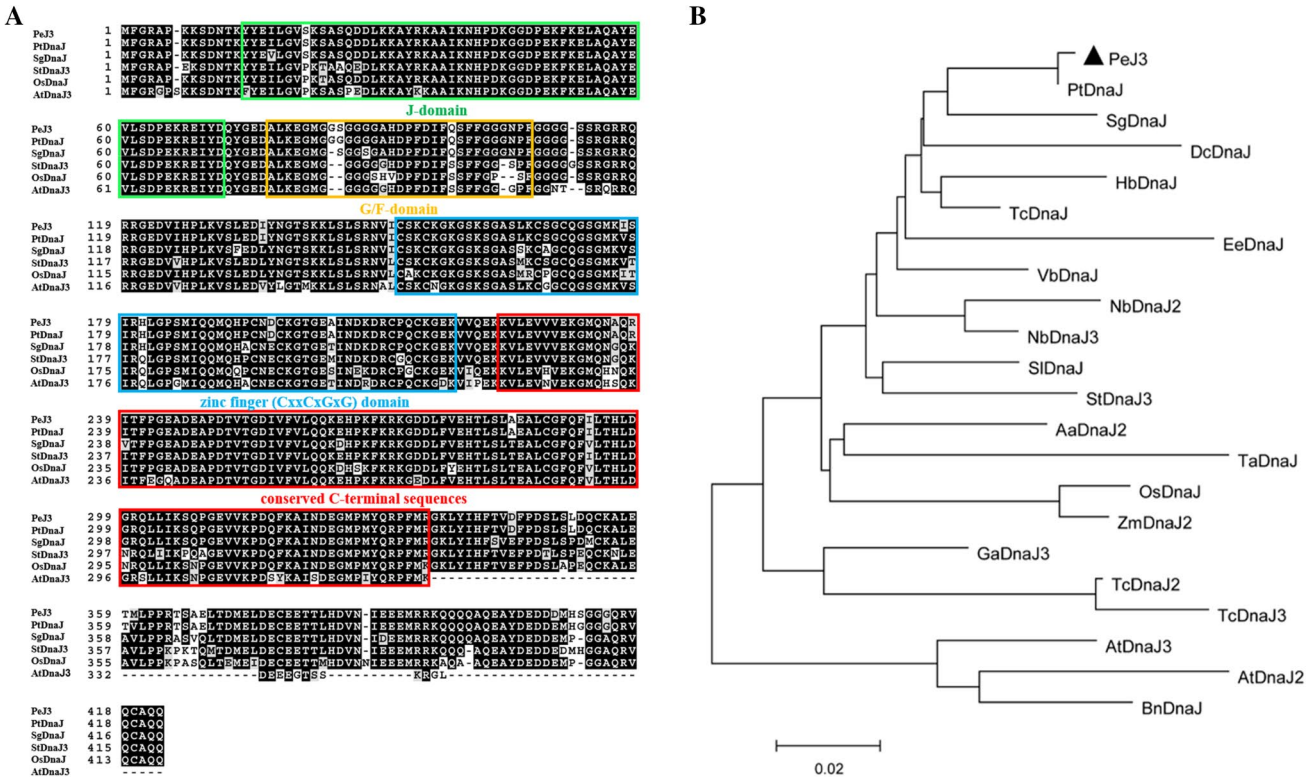

Fig. 2 Multiple sequence alignment and phylogenetic analysis of *P. euphratica* DnaJ3 (PeJ3). **A** Multiple sequence alignment shows PeJ3 compared to other DnaJ proteins from different species. PeJ3 shows a high degree of amino acid homology with DnaJs from other higher-order plants: PtDnaJ, *Populus trichocarpa* DnaJ; SgDnaJ, *Salix gilgiana* DnaJ; StDnaJ3, *Solanum tuberosum* DnaJ3; OsDnaJ, *Oryza sativa Japonica Group* DnaJ; AtDnaJ3, *Arabidopsis thaliana* DnaJ3. *Black and grey shading* indicate identical and conserved amino acid residues, respectively. The protein sequence of PeJ3 contains a J-domain (*green box*), a proximal G/F-domain (*gold box*), and a distal zinc finger (CxxCxGxG) domain (*blue box*), followed by less conserved C-terminal sequences (*red box*). **B** Phylogenetic relationships between the PeJ3 protein sequence and other representative DnaJ proteins from different plant species. The different species are indicated as follows: Pe, *Populus euphratica*; Pt, *Populus trichocarpa*; Sg, *Salix gilgiana*; Dc, *Daucus carota*; Hb, *Hevea brasiliensis*; Tc, *Theobroma cacao*; Ee, *Euphorbia esula*; Vb, *Viola baoshanensis*; Nb, *Nicotiana benthamiana*; Sl, *Solanum lycopersicum*; St, *Solanum tuberosum*; Aa, *Allium ampeloprasum*; Ta, *Triticum aestivum*; Os, *Oryza sativa Japonica Group*; Zm, *Zea mays*; Ga, *Gossypium arboreum*; At, *Arabidopsis thaliana*; Bn, *Brassica napus*. (Color figure online)

Results

NaCl-mediated changes in *PeJ3* and *PePKS5* expression in *Populus euphratica*

The RT-qPCR results showed that NaCl exposure caused a marked rise in *PeJ3* transcription relative to both reference genes, *PeACT7* (Fig. 1A) and *PeACT2*, in *P. euphratica* cells (Supplemental Fig. 2). A 2.54-fold increase in *PeJ3* transcript abundance was observed in the first 12 h of treatment (Fig. 1A). Thereafter, at 24 h, another increase occurred, and *PeJ3* transcript abundance was 4.2-fold higher than controls (Fig. 1A). Those data were consistent with findings in the leaves of NaCl-stressed *P. euphratica* seedlings (Supplemental Fig. 1). This NaCl-mediated increase in *PeJ3* transcripts suggested that PeJ3 was correlated to salinity tolerance in *P. euphratica*.

The Arabidopsis chaperone, J3, was previously shown to interact with PKS5 kinase to regulate the PM H^+-ATPase (Yang et al. 2010). Therefore, we examined *PePKS5* transcripts in *P. euphratica* cells, to determine whether the *PePKS5* transcription pattern differed from the *PeJ3* transcription pattern during the salt response. RT-qPCR data showed that *PePKS5* transcription markedly decreased after 12 h of salt stress (100 mM NaCl; Fig. 1B, Supplemental Fig. 2), and it reached a minimum at the end of salt treatment (24 h, Fig. 1B, Supplemental Fig. 2). These data indicated that NaCl salinity suppressed *PePKS5* expression in *P. euphratica* cells, in contrast to *PeJ3* expression, which was upregulated by salt (Fig. 1, Supplemental Fig. 2). Conversely, KCl (100 mM) exposure did not significantly alter the expression of *PeJ3* or *PePKS5* relative to the two reference genes, *PeACT7* and *PeACT2*, in *P. euphratica* calli (Supplemental Fig. 3).

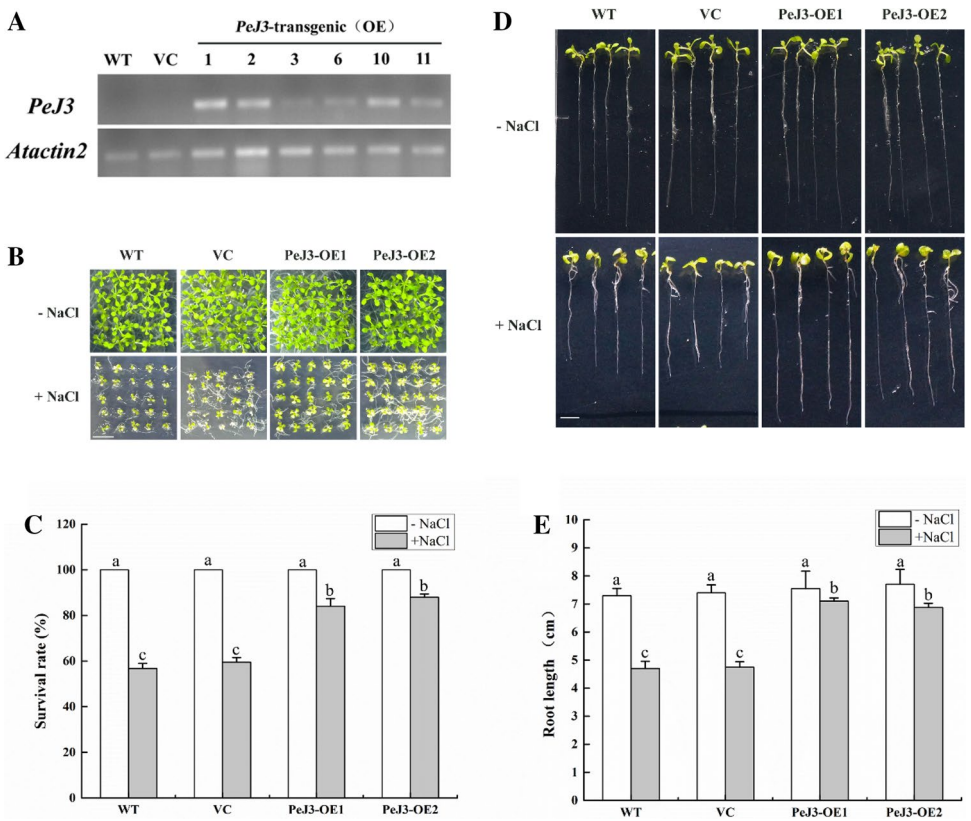

Fig. 3 Salt tolerance tests in wild-type (WT), vector control (VC), and *PeJ3*-transgenic Arabidopsis lines. **A** Semi-quantitative reverse transcription PCR analysis of *PeJ3* overexpression (OE) after transformation. *Atactin2* served as the internal control. Forward and reverse primers are shown in Supplementary Table 1. **B**–**E** Salt tolerance tests in 1/2 MS medium. Seeds from WT, VC and transgenic lines (PeJ3-OE1 and PeJ3-OE2) were allowed to germinate on 1/2 MS medium containing 0 or 100 mM NaCl. Survival rate and root length were measured after 10 days of salt treatment. Representative images show **B** plant survival and **D** root lengths after 10 days in the absence (−) and presence (+) of NaCl stress; *scale bars* 1 cm. Quantitative evaluations of **C** plant survival and **E** root length. *Each column* is the mean of three replicated experiments and *bars* represent the standard error of the mean. *Columns labeled with different letters* (*a, b*, and *c*) denote significant differences ($P < 0.05$) between control (−NaCl) and salt exposure (+NaCl). (Color figure online)

Sequence analysis of PeJ3

The 1269-bp full-length cDNA of *PeJ3* encodes a putative protein of 422 amino acids (Fig. 2A). The PeJ3 sequence displayed high similarity to that of DnaJs from other higher-order plants; e.g., Arabidopsis DnaJ3 (Yang et al. 2010) (Fig. 2A). Furthermore, the PeJ3 protein contains typical DnaJ domains, including the J-domain, the G/F-domain, the zinc finger (CxxCxGxG) domain, and C-terminal sequences that are less conserved (Fig. 2A).

A comparative phylogenetic analysis of PeJ3 with a set of 21 protein sequences indicated that PeJ3 displayed homology to DnaJs from diverse species (Fig. 2B). Accordingly, PeJ3 could be classified as a DnaJ.

Salinity tolerance of *PeJ3*-transgenic plants

Six positive transgenic lines, OE1, OE2, OE3, OE6, OE10, and OE11, were obtained by introducing the *PeJ3* gene into Arabidopsis. These transgenic lines were identified with semi-quantitative reverse transcription PCR and RT-qPCR. As expected, *PeJ3* was not detectable in the WT Arabidopsis or the VC lines (Fig. 3A). PeJ3-OE1 and PeJ3-OE2 showed remarkably higher *PeJ3* transcription levels than the other four transgenic lines (Fig. 3A). The data obtained with semi-quantitative reverse transcription PCR were confirmed with RT-qPCR (Supplemental Fig. 4). Therefore, the PeJ3-OE1 and PeJ3-OE2 transgenic lines were used for further salt tolerance tests. Based on RT-qPCR assays with different endogenous reference genes (*Atactin2*, Fig. 4A; *AtEF1α*, Supplemental Fig. 5), in the PeJ3-OE1 and PeJ3-OE2 transgenic lines, *PeJ3* overexpression had no significant effect on *AtJ3* transcription (Fig. 4A; Supplemental Fig. 5).

AtPKS5 transcription was also examined in PeJ3-OE1 and PeJ3-OE2 transgenic Arabidopsis lines. RT-qPCR data showed that *PeJ3* overexpression suppressed *AtPKS5* transcription in transgenic seedlings (Fig. 4B, Supplemental Fig. 5). Compared to WT, the *AtPKS5* transcript abundance was reduced by 44–48% in both transgenic lines (Fig. 4B).

In salinity tests, the Arabidopsis survival rate was lowered by NaCl (100 mM) after 10 days of treatment. However, the two transgenic lines maintained higher survival rates than WT and VC lines (Fig. 3B, C). Root length was reduced in NaCl-treated plants, but root growth reductions were less severe in transgenic lines (6.6–10.4%) than in WT (35.6%) and VC plants (35.1%, Fig. 3D, E). In this study, PeJ3-OE1 and PeJ3-OE2 seedlings were not significantly different from WT and VC in survival and root growth under control (no salt) conditions (Fig. 3B–E).

A parallel experiment was performed with KCl instead of NaCl to separate any potential conflation with osmotic

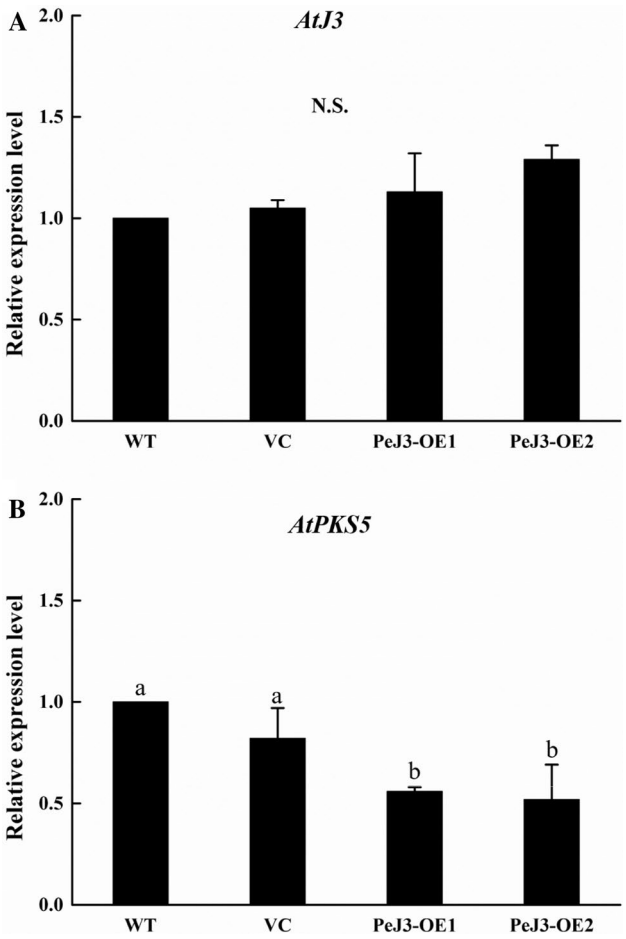

Fig. 4 Effects of *PeJ3* on Arabidopsis expression profiles. RT-qPCR results show relative expression of **A** *AtJ3* and **B** *AtPKS5* in wild-type (WT) Arabidopsis, vector control (VC), and *PeJ3*-transgenic lines (PeJ3-OE1 and PeJ3-OE2). Seeds from WT, VC and *PeJ3*-transgenic (PeJ3-OE1 and PeJ3-OE2) were germinated on 1/2 MS medium. Ten-day-old seedlings of all tested lines were sampled for total RNA extraction and real-time quantitative PCR analysis. *Arabidopsis β-actin 2 (Atactin2)* was used as internal control. Primers designed to target *AtJ3, AtPKS5*, and *Atactin2* are shown in Supplemental Table 1. *Each column* is the mean of three independent experiments and *bars* represents the standard error of the mean. *Columns labeled with different letters* (*a* and *b*) denote significant differences ($P < 0.05$). *N.S.* no significant difference between WT, VC, and *PeJ3*-transgenic lines

effects. Iso-osmotic stress caused by 100 mM KCl did not affect the survival rates of WT, VC, or the two transgenic lines (Supplemental Fig. 6A, B). This finding was distinct from the effects of NaCl (100 mM), which significantly lowered the survival rates of all tested lines (Fig. 3B, C). In addition, KCl treatment resulted in similar root growth among all four tested lines (Supplemental Fig. 6C, D). In contrast, NaCl treatment severely suppressed root growth in WT and VC lines and had less of an effect in the two salt-tolerant transgenic lines (Fig. 3D, E).

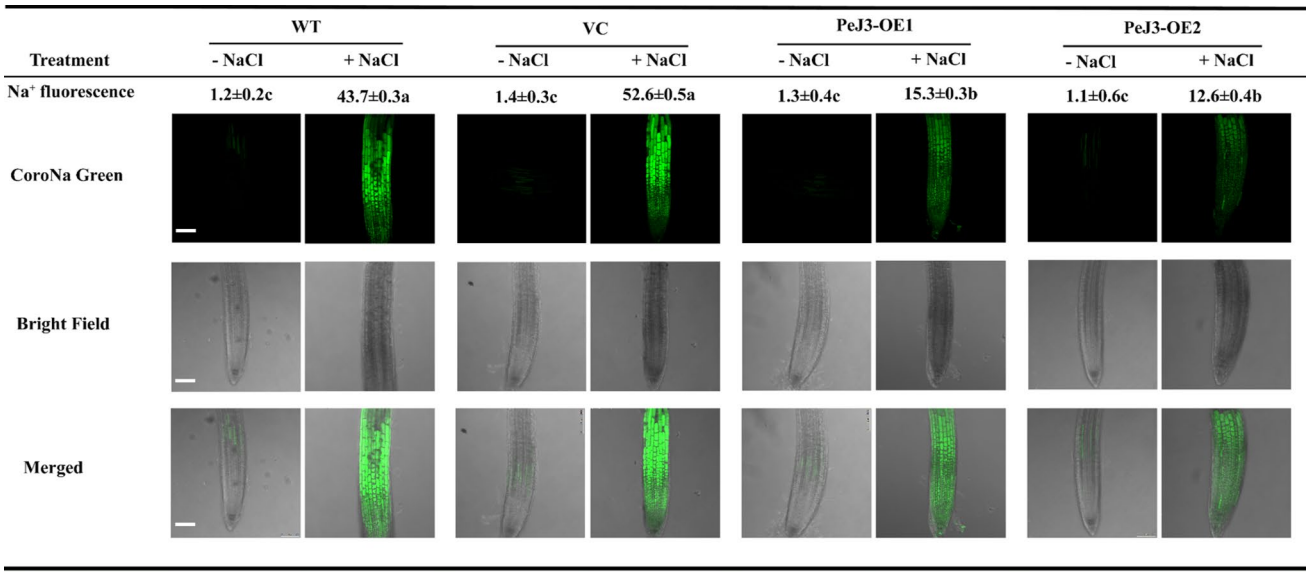

Fig. 5 Na^+ levels in root cells of wild-type (WT) Arabidopsis, vector control (VC), and *PeJ3*-transgenic lines (PeJ3-OE1 and PeJ3-OE2) under NaCl stress. Seven-day-old seedlings were transferred to 1/2 MS medium supplemented with or without 100 mM NaCl for 12 h. Seedlings were then incubated with CoroNa-Green AM (*green*, sodium-specific) for 1 h. *Green fluorescence* within cells was detected at the apical region of roots under a Leica confocal microscope. Representative images show Na^+ content (measured with CoroNa green) in plant roots. The mean fluorescence values labeled with *different letters* (*a, b*, and *c*) denote significant differences ($P < 0.05$) between control (−NaCl) and salt stress (+NaCl) conditions. *Scale bar* 250 μm. (Color figure online)

Na^+ concentrations in roots

CoroNa™ Green was used to detect Na^+ concentrations within root cells. Under control (no salt) conditions, the specific fluorescence intensity was very weak (Fig. 5), indicating that the Na^+ concentration was very low in the roots of all tested genotypes. Root Na^+ concentrations significantly increased after 12 h of salt exposure (100 mM NaCl, Fig. 5). However, the fluorescence intensity in WT and VC plants was nearly threefold higher than that observed in PeJ3-OE1 and PeJ3-OE2 roots (Fig. 5). This finding indicated that the enhanced salt tolerance of PeJ3-transgenic Arabidopsis plants was related to lower Na^+ accumulation in the roots.

NaCl-mediated changes in root Na^+ and K^+ fluxes

The low accumulations of Na^+ in transgenic plants was mostly due to Na^+ extrusion in salinized roots. NMT recordings revealed that Na^+ efflux was significantly increased in PeJ3-OE1 and PeJ3-OE2 roots after 12 h of NaCl stress (100 mM, Fig. 6A). Notably, transgenic lines exhibited fourfold higher Na^+ fluxes than WT and VC plants (Fig. 6A). In addition, we noticed that in control conditions, roots of transgenic lines typically displayed higher Na^+ efflux, compared to WT and VC roots (Fig. 6A).

To explore the role of PeJ3 in K^+ homeostasis, we compared root K^+ fluxes in high NaCl conditions in WT, VC, and transgenic lines. Arabidopsis roots exhibited a steady K^+ influx under control conditions, but PeJ3-OE1 and PeJ3-OE2 roots displayed higher K^+ uptake rates than WT and VC roots (Fig. 6B). Exposure to NaCl reversed the rectification of K^+ from influx to efflux in all tested lines (Fig. 6B). However, the K^+ effluxes were markedly lower in transgenic plants than in WT and VC plants (Fig. 6B).

PM H^+-ATPase activity in *PeJ3*-transgenic Arabidopsis

Transient kinetic recordings revealed that NaCl exposure (100 mM NaCl) elicited H^+ efflux in Arabidopsis roots (Fig. 7A). Of note, *PeJ3*-transgenic plants exhibited a significantly higher rate of H^+ efflux than WT and VC plants (Fig. 7A). However, the salt-induced H^+ efflux shifted to a net influx when sodium vanadate was added in all tested lines (Fig. 7B). This result suggested that the salt-induced H^+ efflux resulted from increased H^+-pumping activity (Sun et al. 2010b; Wang et al. 2013b; Zhao et al. 2016). The fact that H^+ efflux was more pronounced in PeJ3-OE1 and PeJ3-OE2 plants indicated that transgenic plants retained high H^+-pumping activity under NaCl stress.

Furthermore, we examined PM H^+-ATPase activities in WT, VC, and transgenic Arabidopsis in vitro with isolated plasma membrane vesicles. Compared to WT and VC, PeJ3-OE1 and PeJ3-OE2 typically displayed higher ATP-hydrolysis activity (2.6-fold; Fig. 7C). This result indicated that PeJ3 upregulated the activity of PM H^+-ATPase in

transgenic Arabidopsis. This finding was consistent with the in vivo coordination of an increase in H^+-transport activity in *PeJ3*-transgenic Arabidopsis roots (Fig. 7A). Similarly, Yang et al. (2010) showed that AtJ3 could enhance the activity of PM H^+-ATPase in Arabidopsis.

H_2O_2 levels in *PeJ3*-transgenic Arabidopsis roots

NaCl (100 mM) shock resulted in a marked H_2O_2 elevation in the roots of WT, VC, and *PeJ3*-transgenic lines (Fig. 8). However, the salt elicited nearly threefold higher H_2O_2 levels in transgenic lines than in WT and VC lines (Fig. 8). These results indicated that *PeJ3* overexpression promoted H_2O_2 production after exposure to high salt conditions.

Discussion

PeJ3 overexpression enhances salt tolerance in Arabidopsis

PeJ3 was upregulated by NaCl in *P. euphratica* calli and leaves (Fig. 1A, Supplemental Figs. 1, 2). This result was consistent with results from microarray data on poplars that showed differences in salinity tolerance (our unpublished data). NaCl exposure upregulated *PeJ3* transcript abundance in *P. euphratica*, in contrast to the response observed in salt-sensitive *Populus popularis*, which exhibited downregulated transcription (our unpublished data). However, iso-KCl treatment did not alter the transcription of *PeJ3* (Supplemental Fig. 3). Thus, our results suggested that *PeJ3* might contribute to salt adaptation in *P. euphratica*. We found that transgenic *PeJ3* expression markedly increased the ability of Arabidopsis to tolerate salinity. NaCl suppressed survival rates and root lengths less when plants overexpressed *PeJ3* than in WT plants (Fig. 3). Similarly, a previous study showed that ectopic expression of *GsJ11* in Arabidopsis promoted seedling root elongation under alkaline salt treatment ($NaHCO_3$, Song et al. 2017). In the present study, *PeJ3*-overexpressing lines differed from WT in their tolerance to NaCl (Fig. 3), but transgenic and WT plants showed similar responses to iso-KCl (Supplemental Fig. 6). This result indicated that PeJ3 contributed to salt tolerance in plants.

The enhanced capacity to tolerate NaCl exposure depended on the ability to extrude Na^+ and maintain K^+ in transgenic plants (Fig. 6). *PeJ3*-transgenic Arabidopsis accumulated less Na^+ in root cells (Fig. 5), which in part, resulted from a high capacity for Na^+ efflux in roots (Fig. 6A). It is of critical importance for glycophytes to extrude Na^+ under salt stress conditions (Greenway and Munns 2003; Chen and Polle 2010; Horie et al. 2012; Chen et al. 2014; Polle and Chen 2015). Moreover,

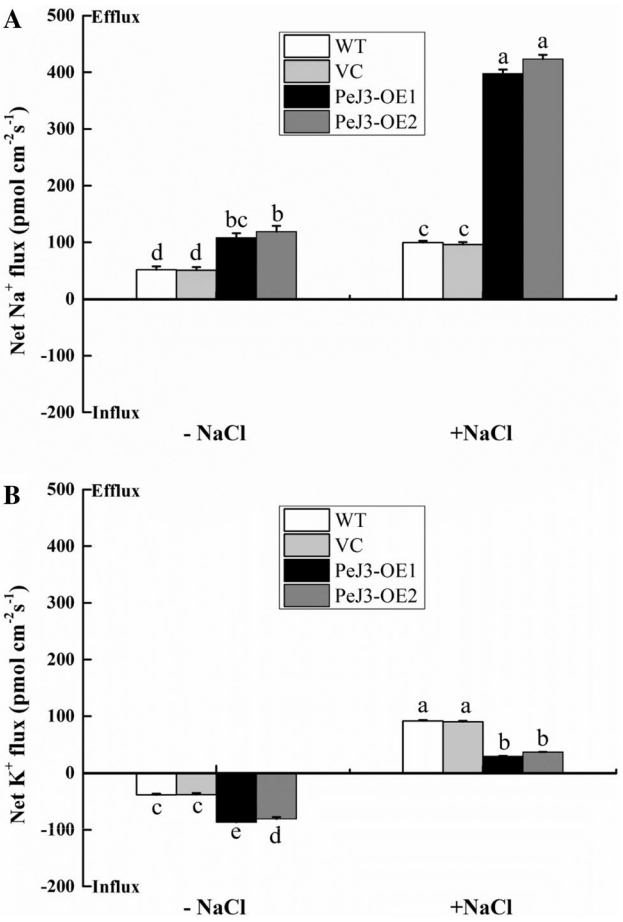

Fig. 6 Effects of PeJ3 on steady-state Na^+ and K^+ fluxes in roots. Net fluxes of **A** Na^+ and **B** K^+ in roots of wild-type (WT) Arabidopsis, vector control (VC), and *PeJ3*-transgenic lines (PeJ3-OE1 and PeJ3-OE2), in control (−NaCl) and salt stress (+NaCl) conditions. Seven-day-old seedlings were transferred to 1/2 MS medium supplemented with or without NaCl (100 mM) for 12 h. Steady-state fluxes of Na^+ and K^+ were continuously recorded for 30 min at the meristematic zone, ca 200 μm from the root apex. *Each column* is the mean of seven independent seedlings, and *bars* represent the standard error of the mean. *Columns labeled with different letters* (*a, b, c, d*, and *e*) denote significant differences ($P < 0.05$) between the tested lines

PeJ3-transgenic plants exhibited greater ability to maintain root K^+ content under salt stress, compared to WT plants (Fig. 6B). It has been repeatedly shown that salt tolerance in crops and woody species was correlated with the capacity to maintain K^+ content (Chen et al. 2005; Cuin et al. 2008; Sun et al. 2009b; Hamdia and Shaddad 2010; Wang et al. 2013a). Electrophysiological evidence from poplars, barley, and wheat cultivars has shown that root K^+ loss induced by NaCl exposure was typically lower in salt-tolerant genotypes, compared to salt-sensitive genotypes (Chen et al. 2005, 2007; Cuin et al. 2008; Sun et al. 2009a, b, 2010b; Shabala et al. 2016). Therefore, PeJ3 benefited stressed Arabidopsis by enhancing the ability to retain K^+/Na^+ homeostasis and withstand ionic toxicity.

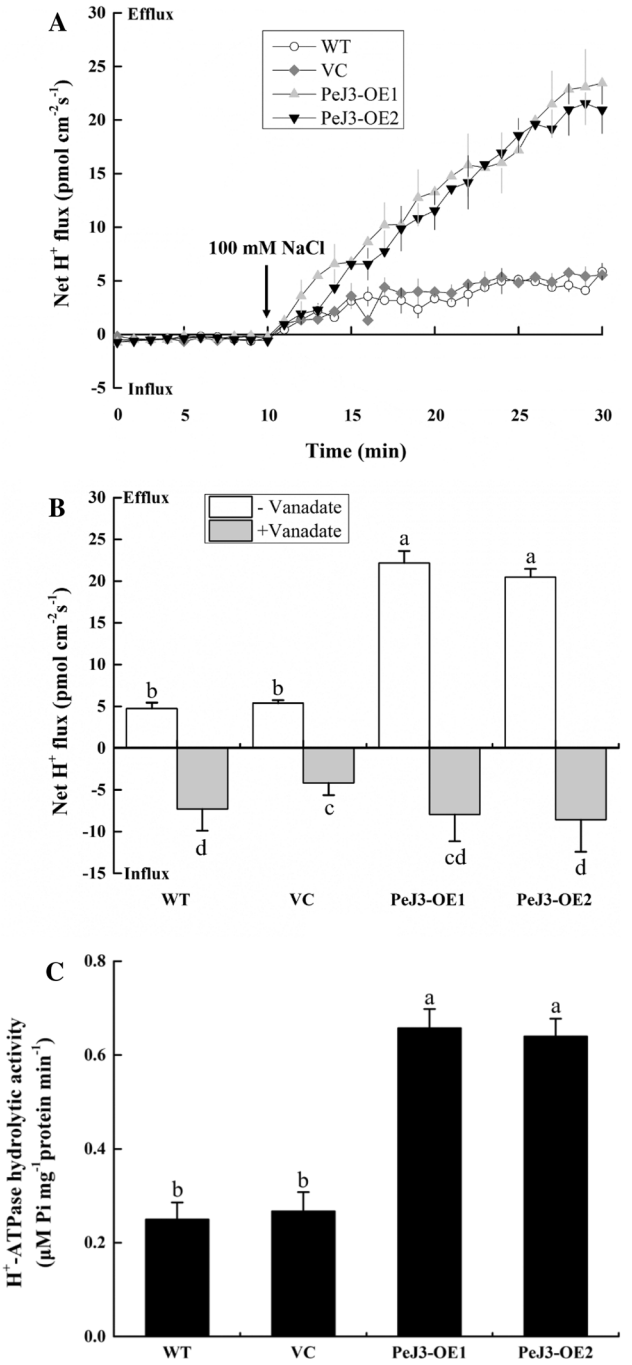

Fig. 7 Transient H^+ kinetics in response to NaCl shock (100 mM) and PM H^+-ATPase activity in Arabidopsis roots. **A** H^+ fluxes in roots before and during 20 min of salt-shock in wild-type (WT) Arabidopsis, vector control (VC), and *PeJ3*-transgenic lines (PeJ3-OE1 and PeJ3-OE2). Prior to the salt shock, steady-state H^+ fluxes were continuously monitored for approximately 10 min. H^+ transient kinetics were recorded after the required amount of 200 mM NaCl stock solution was slowly added to the chamber to yield a final concentration of 100 mM. Each *point* is the mean of seven independent seedlings, and *bars* represent the standard error of the mean. **B** Effects of sodium vanadate on salt shock-induced H^+ fluxes in WT, VC, and *PeJ3*-transgenic lines (PeJ3-OE1 and PeJ3-OE2). All roots were pretreated with 500 μM sodium vanadate for 30 min prior to flux recordings upon NaCl shock. Columns show the mean H^+ flux rates after 20 min of salt shock in Arabidopsis roots in the absence (−Vanadate) or presence (+Vanadate) of inhibitor. *Each column* is the mean of seven independent seedlings, and *bars* represent the standard error of the mean. **C** ATP hydrolysis activity, measured as inorganic phosphate (Pi) production, for PM H^+-ATPase in Arabidopsis. Plasma membrane vesicles were isolated from 4-week-old seedlings of WT, VC and *PeJ3*-transgenic lines (PeJ3-OE1 and PeJ3-OE2). *Each column* is the mean of three independent experiments, and *bars* represent the standard error of the mean. *Columns labeled with different letters* (*a, b, c* and *d*) denote significant differences ($P < 0.05$) between treatments (**B**) or between the tested lines (**C**)

PeJ3 upregulates the activity of PM H^+-ATPase in transgenic Arabidopsis

Enhanced H^+-pumping activity enabled *PeJ3*-transgenic plants to maintain root K^+/Na^+ homeostasis under NaCl stress. In vitro assays revealed that *PeJ3* overexpression upregulated ATP-hydrolysis activity in the PM H^+-ATPase (Fig. 7C). H^+-pumps provide an electrochemical H^+ gradient across the PM (Blumwald et al. 2000; Zhu 2003; Sun et al. 2009a). Moreover, in vivo analyses with NMT recordings showed that *PeJ3*-transgenic plants displayed elevated H^+ efflux under salt stress (Fig. 7A, B). This H^+ efflux was blocked with sodium vanadate, which indicated that high H^+ pump activity was responsible for the elevated H^+ efflux (Sun et al. 2010b; Wang et al. 2013b). These data suggested that transgenic Arabidopsis had generated an intensive proton-driving force for Na^+/H^+ exchange under NaCl stress (Fig. 7A). In addition to promoting Na^+/H^+ exchange, the activated H^+-pumps benefited salinized roots by enhancing K^+ homeostasis (Fig. 6B). The activated H^+ pump is thought to repolarize the plasma membrane, which reduces K^+ loss through DA-KORCs and DA-NSCCs (Shabala et al. 2006, 2016; Sun et al. 2010b). Presumably, the PM H^+-pumps in transgenic plants were activated by PeJ3. AtJ3 was shown to activate the PM H^+-ATPase by directly inhibiting AtPKS5 or modifying AtPKS5 affinity for the proton pump (Yang et al. 2010). The protein sequence of PeJ3 exhibited high similarity to Arabidopsis AtJ3 (Fig. 2). Therefore, it was thought that PeJ3 improved the activity of PM H^+-ATPase in Arabidopsis by interacting with AtPKS5 kinase (Fuglsang et al. 2007; Yang et al. 2010). Moreover, *AtPKS5* transcription was suppressed by *PeJ3* overexpression (Fig. 4B, Supplemental Fig. 5). Therefore, we reasoned that overexpression of *PeJ3* might enhance PM H^+-ATPase activity by suppressing the transcription of *AtPKS5* in Arabidopsis. Song et al. (2017) also showed that *GsJ11* regulated the transcription of the H^+-ATPase. *GsJ11* overexpression in Arabidopsis caused a rapid increase in the transcription levels of H^+-ATPase genes after $NaHCO_3$ treatment, which contributed to PM H^+-ATPase activation and alkaline resistance (Song et al. 2017).

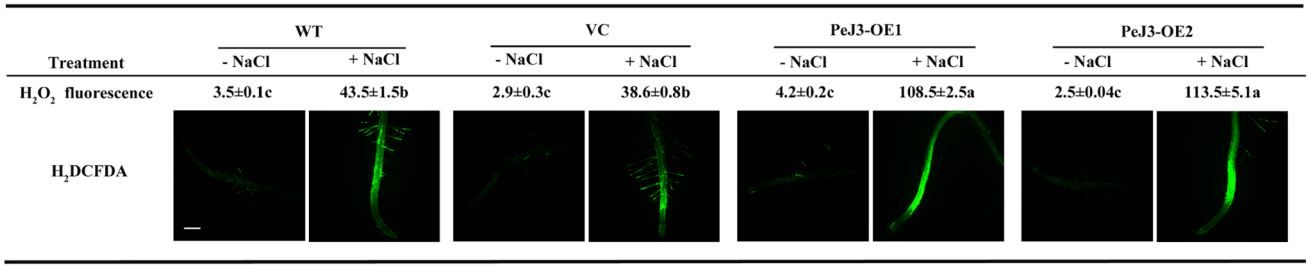

Fig. 8 NaCl stress induced early H_2O_2 production in roots of wild-type (WT) Arabidopsis, vector control (VC), and *PeJ3*-transgenic lines (PeJ3-OE1 and PeJ3-OE2). Seven-day-old seedlings were transferred to 1/2 MS medium supplemented with or without 100 mM NaCl for 10 min. Seedlings were then incubated with H_2DCF-DA for 5 min. Green fluorescence within cells was detected at the apical region of roots under a Leica confocal microscope. Representative images show H_2O_2 content (measured with H_2DCFDA) in plant roots. *Scale bar* 250 µm. The fluorescence intensity (±SD) represents the mean of seven independent seedlings. The mean values of H_2O_2 fluorescence are labeled with *different letters* (*a, b*, and *c*) to denote significant differences ($P<0.05$) between control (−NaCl) and salt treatment (+NaCl). (Color figure online)

Overexpression of *PeJ3* enhances H_2O_2 signaling in salt-stressed Arabidopsis

Upon NaCl shock, transgenic Arabidopsis produced nearly threefold higher H_2O_2 levels in root cells, compared to WT and VC roots (Fig. 8). H_2O_2 serves as a salt signaling molecule in plants (Leshem et al. 2006; Zhang et al. 2007; Moschou et al. 2008; Sun et al. 2010a, b, 2012; Shen et al. 2013). We previously showed that, under NaCl salinity, H_2O_2 production was triggered by proton-coupled ion transporters in the PM; e.g., H^+-pumps and Na^+/H^+ antiporters (Sun et al. 2010b; Wang et al. 2013b). After the NaCl shock, H_2O_2 production increased more rapidly in *PeJ3*-transgenic roots than in WT roots (Fig. 8). The pronounced H^+ efflux driven by the H^+-pumps (Fig. 7) would lead to an acidic pH in the apoplast, which caused activation of NADPH oxidases (Wang et al. 2013b). In *P. euphratica* cells, H_2O_2 was previously shown to increase cytosolic Ca^{2+} and promote Na^+/H^+ exchange (Sun et al. 2010a, b). Therefore, the rapid production of H_2O_2 elicited by salt in *PeJ3*-transgenic Arabidopsis would likely trigger adjustments that benefitted K^+/Na^+ homeostasis.

Conclusion

Based on the characterization of *PeJ3* in transgenic Arabidopsis here, and in our previous reports, we propose that PeJ3 plays an important role in mediating plant K^+/Na^+ homeostasis. The proposed mechanism of action is shown in Fig. 9. The salt induction of *PeJ3* expression resulted in the activation of PM H^+-ATPase, through transcriptional suppression of *PePKS5* and/or interaction with the PePKS5 kinase (Fuglsang et al. 2007; Yang et al. 2010). Subsequently, the activated H^+-pumps (i) promoted Na^+/H^+ exchange across the PM, (ii) reduced K^+ efflux mediated by depolarization-activated channels (e.g., DA-KORCs and DA-NSCCs) in the PM, and (iii) stimulated the H_2O_2 signaling pathway, which involved NADPH oxidase; this pathway increased cytosolic free Ca^{2+} and stimulated Na^+ extrusion through the Salt Overly Sensitive (SOS) signaling pathway.

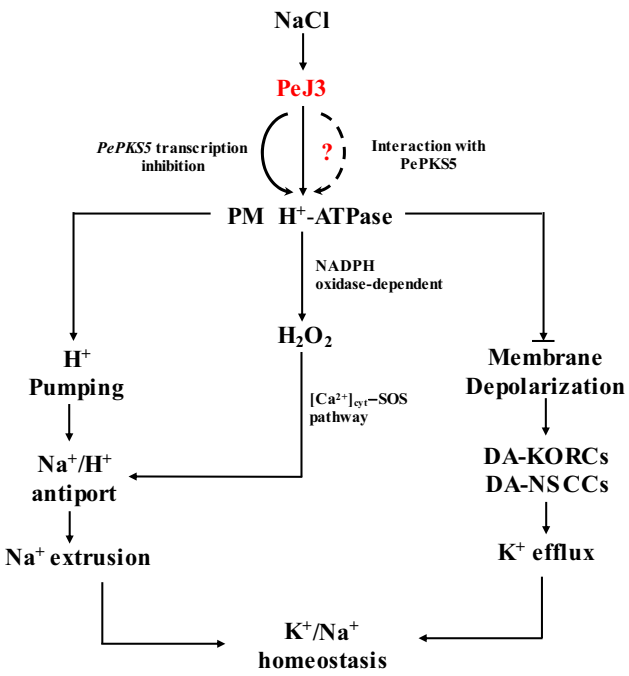

Fig. 9 Schematic model shows the role of PeJ3 in maintaining K^+/Na^+ homeostasis under NaCl stress conditions by activating the PM H^+-ATPase in *Populus euphratica*. *PM* plasma membrane, *SOS* Salt Overly Sensitive signaling pathway, *DA* depolarization activated, *KORCs* K^+ outward rectifying channels, *NSCCs* non-selective cation channels. (Color figure online)

Acknowledgements The research was supported jointly by the Fundamental Research Funds for the Central Universities (Grant No. 2017ZY07), National Natural Science Foundation of China (Grant Nos. 31570587 and 31270654), the Research Project of the Chinese Ministry of Education (Grant No. 113013A), Beijing Natural Science Foundation (Grant No. 6172024), the Program of Introducing Talents of Discipline to Universities (111 Project, Grant No. B13007), and the Program for Changjiang Scholars and Innovative Research Teams in University (Grant No. IRT13047).

Author Contributions Y-NZ, YW, and SC conceived the original screening and research plans; SC, CL, SL, and RZ supervised the experiments; Y-NZ, YW, GS, Y-HZ, and JD performed most of the experiments; SD, MW, HZ, JY, XM, RZ, and XZ provided technical assistance to Y-NZ, YW, GS, Y-HZ, JD; Y-NZ and YW analyzed the experimental data; Y-NZ wrote the article and SC supervised the writing. All coauthors agreed and approved the manuscript.

References

Akbari M, Labeau F (2003) The plasma membrane proton pump ATPase: the significance of gene subfamilies. Planta 216:355–365

Apse MP, Blumwald E (2007) Na^+ transport in plants. FEBS Lett 581:2247–2254

Blumwald E, Aharon GS, Apse MP (2000) Sodium transport in plant cells. Biochim Biophys Acta 1465:140–151

Boston RS, Viitanen PV, Vierling E (1996) Molecular chaperones and protein folding in plants. Plant Mol Biol 32:191–222

Britto DT, Kronzucker HJ (2008) Cellular mechanisms of potassium transport in plants. Physiol Plant 133:637–650

Camoni L, Iori V, Marra M, Aducci P (2000) Phosphorylation-dependent interaction between plant plasma membrane H^+-ATPase and 14-3-3 proteins. J Biol Chem 275:9919–9923

Caplan AJ, Cyr DM, Douglas MG (1993) Eukaryotic homologues of *Escherichia coli* dnaJ: a diverse protein family that functions with hsp70 stress proteins. Mol Biol Cell 4:555–563

Chen S, Polle A (2010) Salinity tolerance of *Populus*. Plant Biol 12:317–333

Chen Z, Newman I, Zhou M, Mendham N, Zhang G, Shabala S (2005) Screening plants for salt tolerance by measuring K^+ flux: a case study for barley. Plant Cell Environ 28:1230–1246

Chen Z, Pottosin II, Cuin TA, Fuglsang AT, Tester M, Jha D, Zepeda-Jazo I, Zhou M, Palmgren MG, Newman IA (2007) Root plasma membrane transporters controlling K^+/Na^+ homeostasis in salt-stressed barley. Plant Physiol 145:1714–1725

Chen S, Hawighorst P, Sun J, Polle A (2014) Salt tolerance in *Populus*: significance of stress signaling networks, mycorrhization, and soil amendments for cellular and whole-plant nutrition. Environ Exp Bot 107:113–124

Chung JS, Zhu JK, Bressan RA, Hasegawa PM, Shi H (2008) Reactive oxygen species mediate Na^+-induced *SOS1* mRNA stability in Arabidopsis. Plant J 53:554–565

Clough SJ, Bent AF (1998) Floral dip: a simplified method for grobacteriummediated transformation of *Arabidopsis thaliana*. Plant J 16:735–743

Cuin TA, Betts SA, Chalmandrier R, Shabala S (2008) A root's ability to retain K^+ correlates with salt tolerance in wheat. J Exp Bot 59:2697–2706

Cuin TA, Bose J, Stefano G, Jha D, Tester M, Mancuso S, Shabala S (2011) Assessing the role of root plasma membrane and tonoplast Na^+/H^+ exchangers in salinity tolerance in wheat: in planta quantification methods. Plant Cell Environ 34:947–961

Ding M, Hou P, Shen X, Wang M, Deng S, Sun J, Xiao F, Wang R, Zhou X, Lu C (2010) Salt-induced expression of genes related to Na^+/K^+ and ROS homeostasis in leaves of salt-resistant and salt-sensitive poplar species. Plant Mol Biol 73:251–269

Foreman J, Demidchik V, Bothwell JH, Mylona P, Miedema H, Torres MA, Linstead P, Costa S, Brownlee C, Jones JD (2003) Reactive oxygen species produced by NADPH oxidase regulate plant cell growth. Nature 422:442–446

Frías I, Serrano R (1996) A major isoform of the maize plasma membrane H^+-ATPase: characterization and induction by auxin in coleoptiles. Plant Cell 8:1533–1544

Fuglsang AT, Guo Y, Cuin TA, Qiu Q, Song C, Kristinasen KA, Bych K, Schulz A, Shabala S, Schumaker KS (2007) *Arabidopsis* protein kinase PKS5 inhibits the plasma membrane H^+-ATPase by preventing interaction with 14-3-3 protein. Plant Cell 19:1617–1634

Gévaudant F, Duby G, Stedingk EV, Zhao R, Morsomme P, Boutry M (2007) Expression of a constitutively activated plasma membrane H^+-ATPase alters plant development and increases salt tolerance. Plant Physiol 144:1763–1776

Greenway AH, Munns R (2003) Mechanisms of salt tolerance in non-halophytes. Annu Rev Plant Biol 31:149–190

Hamdia MA, Shaddad, M. AK (2010) Salt tolerance of crop plants. J Stress Physiol Biochem 6(3):64–90

Han Y, Wang W, Sun J, Ding M, Zhao R, Deng S, Wang F, Hu Y, Wang Y, Lu Y, Du L, Hu Z, Diekmann H, Shen X, Polle A, Chen S (2013) *Populus euphratica* XTH overexpression enhances salinity tolerance by the development of leaf succulence in transgenic tobacco plants. J Exp Bot 64:4225–4238

Han Y, Sa G, Sun J, Shen Z, Zhao R, Ding M, Deng S, Lu Y, Zhang Y, Shen X, Chen S (2014) Overexpression of *Populus euphratica* xyloglucan endotransglucosylase/hydrolase gene confers enhanced cadmium tolerance by the restriction of root cadmium uptake in transgenic tobacco. Environ Exp Bot 100:74–83

Hasegawa PM, Bressan RA, Zhu JK, Bohnert HJ (2000) Plant cellular and molecular responses to high salinity. Annu Rev Plant Physiol Plant Mol Biol 51:463–499

Horie T, Karahara I, Katsuhara M (2012) Salinity tolerance mechanisms in glycophytes: an overview with the central focus on rice plants. Rice 5:11

Janicka-Russak M (2011) Plant plasma membrane H^+-ATPase in adaptation of plants to abiotic stresses. In: Shanker A, Venkateswarlu B (eds) Abiotic stress response in plants—physiological, biochemical and genetic perspectives, Chap. 8. InTech, Rijeka, pp 197–218

Kim YS, Min JK, Kim D, Jung J (2001) A soluble auxin-binding protein, ABP57. Purification with anti-bovine serum albumin antibody and characterization of its mechanistic role in the auxin effect on plant plasma membrane H^+-ATPase. J Biol Chem 276:10730–10736

Kwak JM, Mori IC, Pei ZM, Leonhardt N, Torres MA, Dangl JL, Bloom RE, Bodde S, Jones J, Schroeder JI (2003) NADPH oxidase *AtrbohD* and *AtrbohF* genes function in ROS-dependent ABA signaling in *Arabidopsis*. Embo J 22:2623–2633

Larsson C, Widell S, Kjellbom P (1987) Preparation of high-purity plasma membranes. Methods Enzymol 148C:558–568

Laufen T, Mayer MP, Beisel C, Klostermeier D, Mogk A, Reinstein J, Bukau B (1999) Mechanism of regulation of hsp70 chaperones by DnaJ cochaperones. Proc Natl Acad Sci USA 96:5452–5457

Leshem Y, Melamedbook N, Cagnac O, Ronen G, Nishri Y, Solomon M, Cohen G, Levine A (2006) Suppression of *Arabidopsis* vesicle-SNARE expression inhibited fusion of H_2O_2-containing vesicles with tonoplast and increased salt tolerance. Proc Natl Acad Sci 103:18008–18013

Li GL, Li B, Liu HT, Zhou RG (2005) The responses of *AtJ2* and *AtJ3* gene expression to environmental stresses in Arabidopsis. Acta Photophysiol Sin 31:47–52

Li J, Bao S, Zhang Y, Ma X, Mishra-Knyrim M, Sun J, Sa G, Shen X, Polle A, Chen S (2012) *Paxillus involutus* strains MAJ and NAU mediate K^+/Na^+ homeostasis in ectomycorrhizal *Populus* × *canescens* under sodium chloride stress. Plant Physiol 159:1771–1786

Livak KJ, Schmittgen TD (2001) Analysis of relative gene expression data using real-time quantitative PCR and the $2^{-\Delta\Delta CT}$ method. Methods 25:402–408

Lu Y, Li N, Sun J, Hou P, Jing X, Zhu H, Deng S, Han Y, Huang X, Ma X, Zhao N, Zhang Y, Shen X, Chen S (2013) Exogenous hydrogen peroxide, nitric oxide and calcium mediate root ion fluxes in two non-secretor mangrove species subjected to NaCl stress. Tree Physiol 33:81–95

Merlot S, Leonhardt N, Fenzi F, Valon C, Costa M, Piette L, Vavasseur A, Genty B, Boivin K, Müller A (2007) Constitutive activation of a plasma membrane H^+-ATPase prevents abscisic acid-mediated stomatal closure. Embo J 26:3216–3226

Mittler R, Vanderauwera S, Gollery M, Van BF (2004) Reactive oxygen gene network of plants. Trends Plant Sci 9:490–498

Morsomme P, Boutry M (2000) The plant plasma membrane H^+-ATPase: structure, function and regulation. Biochim Biophys Acta 1465:1–16

Moschou PN, Paschalidis KA, Delis ID, Andriopoulou AH, Lagiotis GD, Yakoumakis DI, Roubelakis-Angelakis KA (2008) Spermidine exodus and oxidation in the apoplast induced by abiotic stress is responsible for H_2O_2 signatures that direct tolerance responses in tobacco. Plant Cell 20:1708–1724

Moshe S, Robert F (2006) Production of reactive oxygen species by plant NADPH oxidases. Plant Physiol 141:336–340

Munns R, Tester M (2008) Mechanisms of salinity tolerance. Annu Rev Plant Biol 59:651–681

Ohnishi T, Gall RS, Mayer ML (1975) An improved assay of inorganic phosphate in the presence of extralabile phosphate compounds: application to the ATPase assay in the presence of phosphocreatine. Anal Biochem 69:261–267

Ottow EA, Polle A, Brosché M, Kangasjärvi J, Dibrov P, Zörb C, Teichmann T (2005) Molecular characterization of PeNhaD1: the first member of the NhaD Na^+/H^+ antiporter family of plant origin. Plant Mol Biol 58:75–88

Oufattole MM, Boutry M (2000) Identification and expression of three new *Nicotiana plumbaginifolia* genes which encode isoforms of a plasma-membrane H^+-ATPase, and one of which is induced by mechanical stress. Planta 210:715–722

Palmgren MG (2001) Plant plasma membrane H^+-ATPases: powerhouses for nutrient uptake. Plant Biol 52:817–845

Palmgren MG, Sommarin M, Serrano R, Larsson C (1991) Identification of an autoinhibitory domain in the C-terminal region of the plant plasma membrane H^+-ATPase. J Biol Chem 266:20470–20475

Polle A, Chen S (2015) On the salty side of life: molecular, physiological and anatomical adaptation and acclimation of trees to extreme habitats. Plant Cell Environ 38:1794–1816

Roberkleber N, Albrechtová JT, Fleig S, Huck N, Michalke W, Wagner E, Speth V, Neuhaus G, Fischeriglesias C (2003) Plasma membrane H^+-ATPase is involved in auxin-mediated cell elongation during wheat embryo development. Plant Physiol 131:1302–1312

Shabala S, Demidchik V, Shabala L, Cuin TA, Smith SJ, Miller AJ, Davies JM, Newman IA (2006) Extracellular Ca^{2+} ameliorates NaCl-induced K^+ loss from *Arabidopsis* root and leaf cells by controlling plasma membrane K^+ -permeable channels. Plant Physiol 141:1653–1665

Shabala L, Zhang J, Pottosin I, Bose J, Zhu M, Fuglsang AT, Velarde-buendia A, Massart A, Hill CB, Roessner U (2016) Cell-type specific H^+-ATPase activity enables root K^+ retention and mediates acclimation to salinity. Plant Physiol 172:2445–2458

Shen Z, Ding M, Sun J, Deng S, Zhao R, Wang M, Ma X, Wang F, Zhang H, Qian Z, Hu Y, Yu R, Shen X, Chen S (2013) Overexpression of *PeHSF* mediates leaf ROS homeostasis in transgenic tobacco lines grown under salt stress conditions. Plant Cell Tiss Organ Cult 115:299–308

Shen Z, Sun J, Yao J, Wang S, Ding M, Zhang H, Qian Z, Zhao N, Sa G, Zhao R, Shen X, Polle A, Chen S (2015) High rates of virus-induced gene silencing by tobacco rattle virus in *Populus*. Tree Physiol 35:1016–1029

Shi HZ, Ishitani M, Cheolsoo K, Zhu JK (2000) The *Arabidopsis thaliana* salt tolerance gene *SOS1* encodes a putative Na^+/H^+ antiporter. Proc Natl Acad Sci 97:6896–6901

Shi H, Lee B, Wu SJ, Zhu JK (2003) Overexpression of a plasma membrane Na^+/H^+ antiporter gene improves salt tolerance in *Arabidopsis thaliana*. Nat Biotechnol 21:81–85

Silver PA, Way JC (1993) Eukaryotic DnaJ homologs and the specificity of Hsp70 activity. Cell 74:5–6

Song X, Duanmu H, Yu Y, Chen C, Sun X, Zhu P, Chen R, Duan X, Li H, Cao L, Nisa Z, Li Q, Zhu Y, Ding X (2017) *GsJ11*, identified by genome-wide analysis, facilitates alkaline tolerance in transgenic plants. Plant Cell Tiss Organ Cult 129:411–430

Sun J, Chen S, Dai S, Wang R, Li N, Shen X, Zhou X, Lu C, Zheng X, Hu Z, Zhang Z, Song J, Xu Y (2009a) NaCl-induced alternations of cellular and tissue ion fluxes in roots of salt-resistant and salt-sensitive poplar species. Plant Physiol 149:1141–1153

Sun J, Dai S, Wang R, Chen S, Li N, Zhou X, Lu C, Shen X, Zheng X, Hu Z, Zhang Z, Song J, Xu Y (2009b) Calcium mediates root K^+/Na^+ homeostasis in poplar species differing in salt tolerance. Tree Physiol 29:1175–1186

Sun J, Li L, Liu M, Wang M, Ding M, Deng S, Lu C, Zhou X, Shen X, Zheng X, Chen S (2010a) Hydrogen peroxide and nitric oxide mediate K^+/Na^+ homeostasis and antioxidant defense in NaCl-stressed callus cells of two contrasting poplars. Plant Cell Tiss Organ Cult 103:205–215

Sun J, Wang MJ, Ding M, Deng S, Liu M, Lu C, Zhou X, Shen X, Zheng X, Zhang Z, Song Z, Hu Z, Xu Y, Chen S (2010b) H_2O_2 and cytosolic Ca^{2+} signals triggered by the PM H^+-coupled transport system mediate K^+/Na^+ homeostasis in NaCl-stressed *Populus euphratica* cells. Plant Cell Environ 33:943–958

Sun J, Zhang X, Deng S, Zhang C, Wang M, Ding M, Zhao R, Shen X, Zhou X, Lu C, Chen S (2012) Extracellular ATP signaling is mediated by H_2O_2 and cytosolic Ca^{2+} in the salt response of *Populus euphratica* cells. PLoS ONE 7(12):e53136

Svennelid F, Olsson A, Piotrowski M, Rosenquist M, Ottman C, Larsson C, Oecking C, Sommarin M (2000) Phosphorylation of Thr-948 at the C terminus of the plasma membrane H^+-ATPase creates a binding site for the regulatory 14-3-3 protein. Plant Cell 11:2379–2391

Wang W, Vinocur B, Shoseyov O, Altman A (2004) Role of plant heat-shock proteins and molecular chaperons in the abiotic stress response. Trends Plant Sci 9:244–252

Wang F, Deng S, Ding M, Sun J, Wang M, Zhu H, Han Y, Shen Z, Jing X, Zhang F, Hu Y, Shen X, Chen S (2013a) Overexpression of a poplar two-pore K^+ channel enhances salinity tolerance in tobacco cells. Plant Cell Tiss Organ Cult 112:19–31

Wang M, Wang Y, Sun J, Ding M, Deng S, Hou P, Ma X, Zhang Y, Wang F, Sa G, Tan Y, Lang T, Li J, Shen X, Chen S (2013b) Overexpression of *PeHA1* enhances hydrogen peroxide signaling in salt-stressed *Arabidopsis*. Plant Physiol Biochem 71:37–48

Waters ER, Vierling E (1996) Evolution, structure and function of the small heat shock proteins in plants. J Exp Bot 47:325–338

Wu Y, Nan D, Xin Z, Zhao M, Chang Z, Liu J, Zhang L (2007) Molecular characterization of *PeSOS1*: the putative Na^+/H^+ antiporter of *Populus euphratica*. Plant Mol Biol 65:1–11

Xing T, Higgins VJ, Blumwald E (1997) Identification of G proteins mediating fungal elicitor-induced dephosphorylation of host plasma membrane H^+ -ATPase. J Exp Bot 48:229–237

Yang Y, Qin Y, Xie C, Zhao F, Zhao J, Liu D, Chen S, Fuglsang AT, Palmgren MG, Schumaker KS (2010) The *Arabidopsis* chaperone J3 regulates the plasma membrane H^+-ATPase through interaction with the PKS5 kinase. Plant Cell 22:1313–1332

Zhang X, Wang H, Takemiya A, Song CP, Kinoshita T, Shimazaki K (2004) Inhibition of blue light-dependent H^+ pumping by abscisic acid through hydrogen peroxide-induced dephosphorylation of the plasma membrane H^+-ATPase in guard cell protoplasts. Plant Physiol 136:4150–4158

Zhang F, Wang Y, Yang Y, Hao WU, Wang DI, Liu J (2007) Involvement of hydrogen peroxide and nitric oxide in salt resistance in the calluses from *Populus euphratica*. Plant Cell Environ 30:775–785

Zhao N, Wang S, Ma X, Zhu H, Sa G, Sun J, Li N, Zhao C, Zhao R, Chen S (2016) Extracellular ATP mediates cellular K^+/Na^+ homeostasis in two contrasting poplar species under NaCl stress. Trees 30:825–837

Zhou RG, Miernyk JA (1999) Cloning and analysis of *AtJ3* gene in *Arabidopsis thaliana*. Acta Bot Sin 41:597–602

Zhu JK (2001) Plant salt tolerance. Trends Plant Sci 6:66–71

Zhu JK (2003) Regulation of ion homeostasis under salt stress. Curr Opin Plant Biol 6:441–445

Zhu JK (2016) Abiotic stress signaling and responses in plants. Cell 167:313–324